Noise-enhanced nonlinear response and the role of modular structure for signal detection in neuronal networks

M. A. Lopes, K.-E. Lee, A. V. Goltsev, and J. F. F. Mendes

Phys. Rev. E **90**, 052709 — Published 12 November 2014

DOI: 10.1103/PhysRevE.90.052709

Noise-enhanced nonlinear response and the role of modular structure for signal detection in neuronal networks

M. A. Lopes,[1] K.-E. Lee,[1] A. V. Goltsev,[1,2] and J. F. F. Mendes[1]

[1] *Department of Physics & I3N, University of Aveiro, 3810-193 Aveiro, Portugal*
[2] *A.F. Ioffe Physico-Technical Institue, 194021 St. Petersburg, Russia*

We show that sensory noise can enhance the nonlinear response of neuronal networks, and when delivered together with a weak signal, it improves the signal detection by the network. We reveal this phenomenon in neuronal networks that are in a dynamical state preceding a saddle-node bifurcation corresponding to the appearance of sustained network oscillations. In this state, even a weak subthreshold pulse can evoke a large-amplitude oscillation of neuronal activity. The signal-to-noise ratio reaches a maximum at an optimum level of sensory noise, manifesting stochastic resonance (SR) at the population level. We demonstrate SR by use of simulations and numerical integration of rate equations in a cortical model. Using this model, we mimic the experiments of Gluckman *et al.* [B. J. Gluckman et al., Phys. Rev. Lett. **77**, 4098 (1996)] that have given evidence of SR in mammalian brain. We also study neuronal networks in which neurons are grouped in modules and every module works in the regime of SR. We find that even a few modules can strongly enhance the reliability of signal detection in comparison with the case when a modular organization is absent.

PACS numbers: 05.10.-a, 05.40.-a, 87.18.Sn, 87.19.ln

I. INTRODUCTION

Noise is ubiquitous in sensory systems and strongly affects their function [1, 2]. Many investigations have been devoted to the problem of how sensory systems compensate, counter or account for noise in order to detect and process sensory information. Stochastic resonance (SR) is recognized as a possible mechanism that allows sensory systems to use noise for its own benefit [1–3]. This phenomenon manifests itself in an amplification and an optimization of weak signals by noise [4]. In the brain, SR was observed in sensory systems [5–8], in central neurons such as hippocampal CA1 neurons in rat cortex [9–11], in the human blood pressure regulatory system [12], and the human brain's visual processing area [13]. SR is also considered as a mechanism mediating neuronal synchronization within and between functionally relevant brain areas [14–16]. At the present time, the understanding the role of SR in brain functioning remains elusive.

Most of the theoretical works on SR, including the seminal paper [17], and experimental realizations of SR refer to systems based on the motion of a particle subjected to a weak periodic signal in a bistable potential [4]. Another mechanism of SR was revealed in a class of dynamical systems based on excitable dynamics [18, 19]. A key ingredient of these systems is that if the system is kicked by a stimulus from its 'rest state' above an activation threshold, then it returns to the state deterministically, within a certain refractory time [18–20]. Based on these ideas, several single neuron models have been proposed to explain SR observed in the brain [6, 10, 11, 19, 21].

SR was also observed at the level of an entire sensory system, i.e., as a collective phenomenon. Gluckman *et al.* [9] revealed a resonance in the response of a neuronal network from mammalian brain on a weak periodic electric stimulus with a certain magnitude of the stochastic component. Since no manifestation of SR at the single cell level was clearly seen in these experiments, one can assume that the observed SR has another nature. Until now, no theoretical explanation of these experiments was proposed. There are some studies of SR in arrays of neurons [22, 23] and summing networks [24], but they did not study the role of interactions between neurons. Pacemaker-driven SR [25, 26] was observed in complex networks of interacting excitable units modeled by Rulkov's discrete map. Also, evidences for SR were found in simulations of small networks of interacting Hodgkin-Huxley neurons [27, 28] and in hippocampal CA3-CA1 networks [29]. Actually, small networks (at most 300 neurons in these papers) do not allow to study collective phenomena due to finite-size effects that manifest themselves in strong irregular fluctuations destroying synchronized activity of neurons. Their impact on critical fluctuations of neuronal activity was recently analyzed in [30]. The breaking of collective phenomena by finite-size effects is a well known phenomenon in physical systems [31, 32], but these effects are still poorly understood in the dynamics of neuronal networks.

In this paper, we propose a mechanism of SR that is based on excitable dynamics of neuronal networks and caused by interaction between neurons rather than excitable dynamics of single neurons. Using simulations of a cortical model of large neuronal networks with stochastic neurons [30, 33] and numerical integration of dynamical equations, we show that, even weak subthreshold (periodic or pulsed) sensory signals can generate correlated activity of a large fraction of neurons in the presence of sensory noise. The signal-to-noise ratio reaches a maximum at an optimum level of sensory noise, manifesting stochastic resonance at the population level. We mimic the experiments of Gluckman *et al.* [9] and we find qualitative agreement with the data. Moreover, we discuss the role of modular organization in the detection of weak signals. For this purpose, we study networks where neu-

rons are grouped in modules and every module works in the regime of SR. We demonstrate that, in this case, the reliability of signal detection is strongly enhanced in comparison with the case when modular organization is absent. We show that when the size of modules decreases, finite-size effects manifest themselves in an increase of activity fluctuations that destroy collective synchronized activity of neurons in the modules.

II. CORTICAL MODEL

In this section, we describe the cortical model, which we use to study SR in neuronal networks. The model was introduced in [33] and generalized to the case of shot noise in [30]. A similar model was proposed in [34, 35] (differences between these models have been discussed in [30]).

A. Structure and rules of stochastic dynamics

We consider neuronal networks composed of stochastic excitatory and inhibitory neurons. The total number of neurons is N, the fraction of excitatory neurons is g_e, and the fraction of inhibitory neurons is $g_i = 1 - g_e$. The neurons are connected by directed edges (synapses) at random with the probability c/N where c is the mean number of synaptic connections. This network has the structure of the Erdős-Rényi network with the Poisson degree distribution. The neurons are bombarded by a flow of random delta-like spikes that represent spontaneous releases of neurotransmitters in synapses and random spikes arriving from other areas of the brain (for example, the activity of the hippocampal CA3 network that causes membrane potential fluctuations in CA1 pyramidal cells like in the model [29]). This flow has properties of shot noise if the spike duration is sufficiently small. The intensity of this flow strongly influences on network dynamics and plays the role of the control parameter in the cortical model [30].

Neurons also receive spikes from active presynaptic excitatory and inhibitory neurons. The total input $I(t)$ at time t to a neuron is the sum of three contributions: (i) random spikes from shot noise, (ii) spikes from excitatory neurons, and (iii) spikes from inhibitory neurons. The input V_j to a neuron with index j, $j = 1, 2, \dots N$, is the integral of $I_j(t)$ over the time interval $[t - \tau, t]$,

$$V_j(t) = nJ_n + kJ_e + lJ_i, \tag{1}$$

where n, k, and l are the numbers of spikes arriving during the time interval $[t - \tau, t]$ from shot noise, active presynaptic excitatory and inhibitory neurons, respectively. J_n is the amplitude of the shot noise spikes. J_e and J_i are the efficacies of synapses from excitatory and inhibitory neurons, respectively.

The dynamics of the stochastic neurons is determined by the following rules. If during the integration time window τ the total input $V_j(t)$ to an inactive neuron becomes larger than a threshold value Ω, then with the probability $\tau\mu_a$ the neuron becomes active and fires a spike train with a constant frequency ν (the index $a = e$ if the neuron is excitatory and $a = i$ if it is inhibitory). If the total input $V_j(t)$ of an active excitatory (inhibitory) neuron becomes smaller than Ω, then the neuron stops to fire with the probability $\tau\mu_a$. In this model, the rates μ_e and μ_i are the reciprocal first-spike latencies of excitatory and inhibitory neurons, respectively. If the ratio

$$\alpha \equiv \mu_i/\mu_e \tag{2}$$

is smaller than 1 then it means that excitatory neurons respond faster to stimuli than inhibitory neurons.

B. Rate equations

The fractions $\rho_e(t)$ and $\rho_i(t)$ of active excitatory and inhibitory neurons, respectively, at time t characterize the neuronal activity in the cortical model. They are determined by the following rate equations [30, 33]:

$$\frac{\dot{\rho_a}}{\mu_a} = -\rho_a + \Psi_a(\rho_e, \rho_i), \tag{3}$$

where $a = e, i$, $\dot{\rho} \equiv d\rho/dt$. The function $\Psi_a(\rho_e, \rho_i)$ is the probability that, at time t, the total input to a randomly chosen excitatory ($a = e$) or inhibitory ($a = i$) neuron is at least the threshold Ω. The function $\Psi_a(\rho_e, \rho_i)$ is determined by the network structure, the distribution function of shot noise (we consider the Gaussian distribution for simplicity), and the frequency-current relationships for single neurons (the step function in our model). Note that the probability $\Psi_a(\rho_e, \rho_i)$ is the same for both excitatory and inhibitory neurons because, in the network under consideration, excitatory and inhibitory neurons occupy topologically equivalent positions. Therefore, $\Psi_e(\rho_e, \rho_i) = \Psi_i(\rho_e, \rho_i) \equiv \Psi(\rho_e, \rho_i)$, where

$$\Psi(\rho_e, \rho_i) = \textstyle\sum_{n,k,l\geq 0} \Theta(nJ_n + J_e k + J_i l - \Omega) G(n) \times P_k(g_e\rho_e\tilde{c}) P_l(g_i\rho_i\tilde{c}). \tag{4}$$

Here, $\tilde{c} = c\nu\tau$, $\Theta(x)$ is the Heaviside step function, $P_k(c)$ is the Poisson distribution function,

$$P_k(c) = c^k e^{-c}/k!, \tag{5}$$

and $G(n)$ is the Gaussian distribution function,

$$G(n) = G_0 e^{-(n-\langle n\rangle)^2/2\sigma^2}. \tag{6}$$

$G(n)$ is the probability that a neuron receives n random spikes from shot noise during the integration time τ. $\langle n\rangle$ is the mean number of these spikes, σ^2 is the variance, and G_0 is the normalization constant, $\sum_{n=0}^{\infty} G(n) = 1$. Note that Eqs. (3) and (4) are asymptotically exact in the limit $N \to \infty$ [30, 33]. They are similar to the phenomenological Wilson-Cowan equations [36, 37] (see a

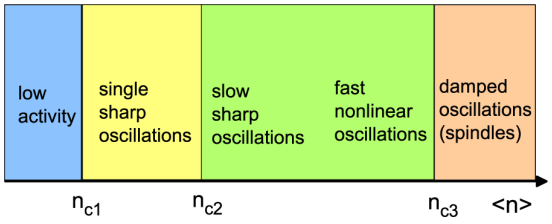

FIG. 1. (Color online) Phase diagram of the cortical model in dependence on the flow intensity $\langle n\rangle$ of random spikes bombarding neurons in the case when excitatory neurons respond faster to input than inhibitory neurons ($\alpha = 0.7$) (adapted from [30]). Stochastic resonance takes place in the region $n_{c1} < \langle n\rangle < n_{c2}$ preceding the saddle-node bifurcation at $\langle n\rangle = n_{c2}$. Above n_{c2} sustained network oscillations appear.

discussion in [33]). The activities ρ_e and ρ_i are comparable to electroencephalographic recordings (EEG), or local field potentials (LFP), representing the activity of thousands of neurons.

In numerical simulations, we use the algorithm proposed in [30] and the following model parameters: $N = 10^4$, $c = 10^3$, $\Omega = 30$, $\tau\nu = 1$, $\mu_e\tau = 0.1$, $\alpha = 0.7$, $g_e = 0.75$ and $g_i = 0.25$. Throughout this paper we use $1/\mu_e \equiv 1$ as time unit and $J_e \equiv 1$ as input unit. Following [38], we consider balanced networks with $J_i = -3J_e$. We also use $J_n = J_e$ and $\sigma^2 = 10$ for the amplitude and the variance of shot noise.

C. Excitable dynamics in the region with stochastic resonance

Now we discuss the excitable dynamics in the region with SR (the region with single sharp oscillations in Fig. 1). At a low noise intensity, $\langle n\rangle < n_{c1}$, the neuronal network is in a state with a low neuronal activity and a weak response to stimuli. Above n_{c1}, in the region $n_{c1} < \langle n\rangle < n_{c2}$, the network demonstrates a peculiar excitable dynamics (the critical points n_{c1} and n_{c2} are defined in [30]). It still relaxes exponentially to the rest state with low activity if a perturbation of neuronal activity is sufficiently weak. However, if a perturbation caused by a pulse is larger than an activation threshold, then a strongly synchronized neuronal activity emerges in the form of a single sharp oscillation. This single sharp oscillation has a large amplitude, it is deterministic and strongly nonlinear. The activation threshold of this sharp oscillation depends on the shot noise intensity $\langle n\rangle$. For example, in the considered network of 10^4 neurons (7500 excitatory and 2500 inhibitory neurons), at $\langle n\rangle = 16$, below $n_{c2} = 18.8$ but above $n_{c1} = 7.6$, the simultaneous activation of only 75 excitatory neurons chosen at random among 7500 excitatory neurons (i.e., about 1% of excitatory neurons), while the other neurons are inactive at that moment, generates a single sharp oscillation formed by the synchronized activity of about 9000 neurons (nature and properties of these nonlinear oscillations are discussed in detail in [30]). The activation threshold decreases when $\langle n\rangle \to n_{c2}$ and finally it becomes zero in the bifurcation point. Due to the small value of the activation threshold, a subthreshold signal together with sensory noise can overcome the threshold and generate a large-amplitude spike of neuronal activity. This kind of excitable dynamics is similar to one discussed within single neuron models [6, 10, 11, 19, 21].

III. STOCHASTIC RESONANCE IN THE CORTICAL MODEL

In this section, using excitable dynamics described in Sec. II C, we demonstrate SR in neuronal networks and mimic SR observed in [9]. In our numerical calculations and simulations, we assume that the first-spike latencies $1/\mu_e$ and $1/\mu_i$ of excitatory and inhibitory neurons equal to 20 ms and 28.6 ms, respectively. Note that the first spike latency is ranged from 25 to 49 ms for CA3 hippocampal pyramidal (excitatory) neurons [39] and from 20 to 128 ms for inhibitory cerebellar stellate cells [40]. For the parameters chosen in Sec. II B and the noise intensity $\langle n\rangle = 25$ corresponding to 12.5 random spikes per second from a synaptic connection, the frequency of sustained network oscillations is about 5.2 Hz. This frequency lies in the range of theta waves [41].

A. SR in numerical integration

Let us study the response of the cortical model to a weak periodic stimuli when the neuronal network is in the regime with excitable dynamics described in Sec. II C. In our numerical integration of Eq. (3), the neuronal network is stimulated by a sensory stimulus $x(t)$ that contains both sensory noise $\xi(t)$ and a periodic signal $S(t)$,

$$x(t) = \xi(t) + S(t). \tag{7}$$

We assume that the sensory stimulus is delivered by $N_s = g_sN_e = g_sg_eN$ sensory neurons, where g_s is a model parameter. These additional sensory neurons are connected at random with the probability c/N only to excitatory neurons. Therefore, each excitatory neuron receives in average an input from g_sg_ec sensory neurons. This method of stimulation assumes that excitatory neurons receive the same signal+noise inputs Eq. (7). It is similar to the experimental method in [9] where all neurons were stimulated by the same electric field.

One can show that the introduction of the sensory neurons leads to a simple modification of Eq. (3). Namely, in Eq. (3), we must substitute the function $\Psi(\rho_e, \rho_i)$ by $\Psi(\rho_e + A_e(t), \rho_i)$ where $A_e(t) = x(t)g_s/(\nu\tau)$. We also introduce an additional stochastic force $F(t)$ acting on neurons and representing other sources of noise different from shot and sensory noise (for example, the force can represent irregular fluctuations caused by finite-size

effects [30, 42]). Equation (3) takes a form,

$$\frac{\dot{\rho_a}}{\mu_a} = (1-\rho_a)F(t) - \rho_a + \Psi(\rho_e + A_e(t), \rho_i). \quad (8)$$

We consider the sensory noise $\xi(t)$ generated by the Gaussian process with the mean number $\langle \xi(t) \rangle = 4 \times 10^{-2}$ of random spikes per the integration time τ and the variance $\sigma_{sn}^2 = 7.3 \times 10^{-4}$ (we only use the positive part of this Gaussian process and the effective mean amplitude of noise, A_ξ, is 4.3×10^{-2}) (see Fig. 2(c)). The sensory signal is sinusoidal,

$$S(t) = A_s[\sin(2\pi f_s t) + 1]/2, \quad (9)$$

with the amplitude $A_s = 4.5 \times 10^{-3}$ and the frequency $f_s = 1.25$ Hz. The ratio $A_s/\langle \xi(t) \rangle$ is close to the value used in [9]. The stochastic force $F(t)$ representing finite-size effects is a random variable uniformly distributed in the interval $[0, 0.009]$.

Analyzing the dynamics of the cortical model by use of Eq. (8), we find that, in the absence of a periodic signal, the sensory noise produces occasionally sharp oscillations. Adding a sinusoidal subthreshold sensory signal, which alone can not generate network oscillations (see Fig. 2(b)), we find that sharp spikes appear preferentially near the maximums of the signal (see Fig. 2(d)).

Following the analysis of Gluckman *et al.*, we find the burst probability density (BPD) defined as the probability to observe a burst (a sharp spike in our case) of network activity when the sinusoidal signal $S(t)$ has a phase ϕ (the signal maximums take place at $\phi = \pi(2n+1)/2$, where $n = 0, 1, \dots$). Figure 3 displays the BPD of the neuronal network at different levels of sensory noise. One can see that the BPD correlates with the sensory signal (see Fig. 3(c)) around an optimal level of sensory noise, while no correlations were observed at weaker or stronger levels of sensory noise (see Figs. 3(b) and (d), respectively). These results agree with the results in [9].

The signal-to-noise ratio (SNR) is defined as follows:

$$SNR = \frac{a}{b} \quad (10)$$

where a is the amplitude of the peak of the power spectral density (PSD) of neuronal activity at the signal's frequency f_s and b is the average value of the background PSD excluding the peak. This method is the same as the one in [9]. The only difference is that in [9] the SNR was defined as $SNR = (a-b)/b$. We apply the periodic sinusoidal signal plus noise to the network as discussed above and then analyze the PSD of the neuronal activity. Results of numerical integration of Eq. (8) and estimation of the SNR for different levels of mean sensory noise are displayed in Fig. 4. The error bars represent the statistics: for each level of noise, we repeat 10 times the measurements of the response of the neuronal network. The maximum of the SNR at a nonzero level of noise in Fig. 4 is a fingerprint of stochastic resonance.

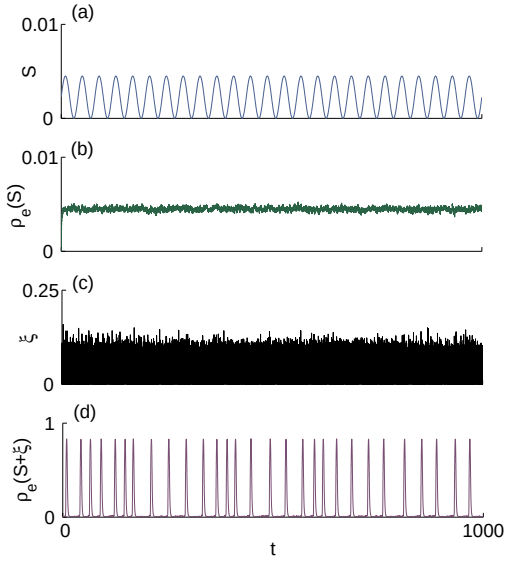

FIG. 2. (Color online) In the absence of sensory noise, a periodic sensory signal (S) with the amplitude $A_s = 4.5 \times 10^{-3}$ (see panel (a)) generates a weak perturbation of the excitatory population activity ρ_e that can hardly be identified in panel (b). However, the addition of sensory noise ξ with the mean amplitude $A_\xi = 4.3 \times 10^{-2}$ (see panel (c)), which is about 10 times larger than the signal's amplitude A_s, results in neuronal activity with single sharp oscillations shown in panel (d). The single sharp oscillations appear preferentially near the peaks of the sensory signal. Network parameters: $c = 1000$, $\Omega = 30$, $g_i = 0.25$, $J_i = -3J_e$, $\sigma^2 = 10$, $\langle n \rangle = 10$, $\alpha = 0.7$, $g_s = 0.1$, and $f_s = 1.25$ Hz. Time t is in units $1/\mu_e$.

B. SR in simulations

In our simulations we considered another stimulation method. The sensory noise and the sinusoidal signal (Eqs. (7) and (9)) were delivered directly to a fraction g_s of $g_e N$ excitatory neurons chosen at random. Sensory noise ξ was represented by random spikes with the mean number $\langle \xi \rangle$ of spikes per the integration time τ and the variance σ_{sn}^2. The amplitude A_s of the sinusoidal signal $S(t)$ was fixed while the level $\langle \xi \rangle$ of sensory noise was gradually increased. Note that there is a simple approximate relationship between $\langle \xi \rangle$ and the noise amplitude A_ξ used in Sec. III A, $\langle \xi \rangle \propto cA_\xi$. We used the amplitude of the sinusoidal signal $A_s = 4.5$ as in the numerical integration. Other model parameters were the same as those in Sec. III A, except $\langle \xi \rangle$ and the variance ($\sigma_{sn}^2 = 5$).

Results of our simulations for $N = 10^4$ are represented in Figs. 5 and 6. At a small level $\langle \xi \rangle$ of sensory noise ($\langle \xi \rangle \leq 5$), the response of the neuronal network to the sinusoidal sensory signal is weak since the probability of generation of sharp oscillations by the signal is small (see Fig. 5(a)). When the level $\langle \xi \rangle$ of sensory noise is increased, sharp oscillations are generated with a larger probability. Note that the degree of correlation of the

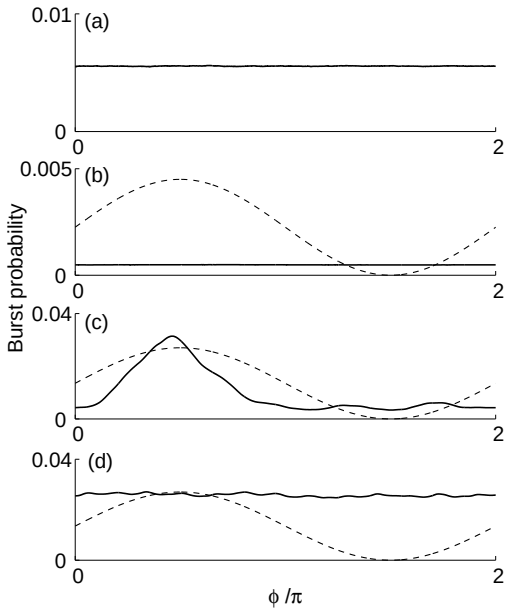

FIG. 3. Burst probability density (BPD) versus the phase ϕ of the sinusoidal sensory signal from the numerical integration of Eq. (8). (a) The BPD versus ϕ in the presence of sensory noise with the mean amplitude $A_\xi = 4.3 \times 10^{-2}$ when the signal is very weak ($A_s \ll A_\xi$). (b) BPD versus ϕ at sensory noise $A_\xi = 2.4 \times 10^{-2}$. (c) BPD at the optimal level of sensory noise $A_\xi = 4.3 \times 10^{-2}$. (d) BPD at strong sensory noise, $A_\xi = 7.0 \times 10^{-2}$. The signal's amplitude $A_s = 4.5 \times 10^{-3}$ is the same for (b), (c), and (d). The data were obtained by averaging over 2500 periods of the signal. The dashed lines represent the signal versus ϕ. Other parameters are the same as in Fig. 2.

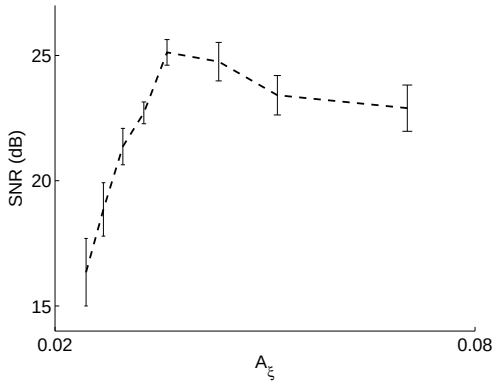

FIG. 4. Signal-to-noise ratio (SNR) versus the mean amplitude A_ξ of the sensory noise in the cortical model from numerical integration of Eq. (8). SNR is in decibel $[10 \log_{10}(SNR)]$. Error bars were estimated from rms distribution of 10 measurements. The bar length is equal to twice the standard deviation. The middle point of the bar corresponds to the mean value of SNR. Parameters are the same as those in Fig. 2.

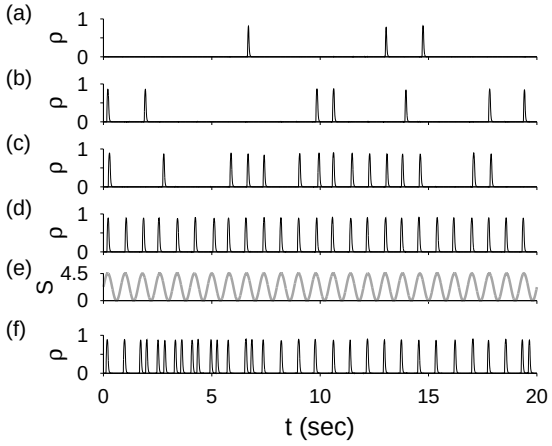

FIG. 5. (Color online) Response of the cortical model of neuronal networks to the sinusoidal sensory signal $S(t)$ at different levels $\langle\xi\rangle$ of sensory noise: (a) $\langle\xi\rangle = 5.0$; (b) $\langle\xi\rangle = 5.5$; (c) $\langle\xi\rangle = 6.0$; (d) $\langle\xi\rangle = 7.0$; (e) sinusoidal signal $S(t)$; (f) $\langle\xi\rangle = 7.5$. Parameters: $A_s = 4.5$ and $\sigma^2_{sn} = 5$. Other parameters in simulations are the same as in Fig. 2.

sharp oscillations with the sensory signal also increases. At the optimum level of sensory noise ($\langle\xi\rangle \approx 7$), the network response (Fig. 5(d)) is well synchronized with the sensory signal (Fig. 5(e)). This synchronization is remarkable since only 10% of excitatory neurons receive the signal+noise input and the level of sensory noise is larger than the signal's amplitude. With increasing $\langle\xi\rangle$ above the optimum level, the correlation between the signal and the network response becomes worse (see Fig. 5(f)).

In order to characterize the network response, we also measured the power spectral density of activity fluctuations and calculated the SNR from Eq. (10). Figures 6(a) and (b) show the PSD of the neuronal activity displayed in Fig. 5(d). One sees that the PSD has a strong peak at the frequency of the sinusoidal signal $S(t)$ (other peaks correspond to the respective harmonics). The amplitude of this peak characterizes the network response. With increasing the level $\langle\xi\rangle$ of sensory noise, the peak increases in comparison with the background amplitude of the PSD, and consequently the SNR increases (see Fig. 6(c)). The SNR reaches a maximum at the optimal noise and then decreases. Again, the inverted-U shape of the SNR is a hallmark of stochastic resonance.

Comparing Figs. 4 and 6(c), one sees that the different methods of stimulation of neurons by signal+noise inputs, which were used in our numerical integration and simulations, give a similar behavior of the SNR. A quantitative comparison of the optimum noise levels in these two different methods is not simple since in numerical calculations we stimulated all excitatory neurons by a signal+noise input from a small group of sensory neurons while in simulations we delivered the signal+noise directly to a small fraction of excitatory neurons. Another reason for this difference is due to strong activity fluctuations caused by finite-size effects. This kind of

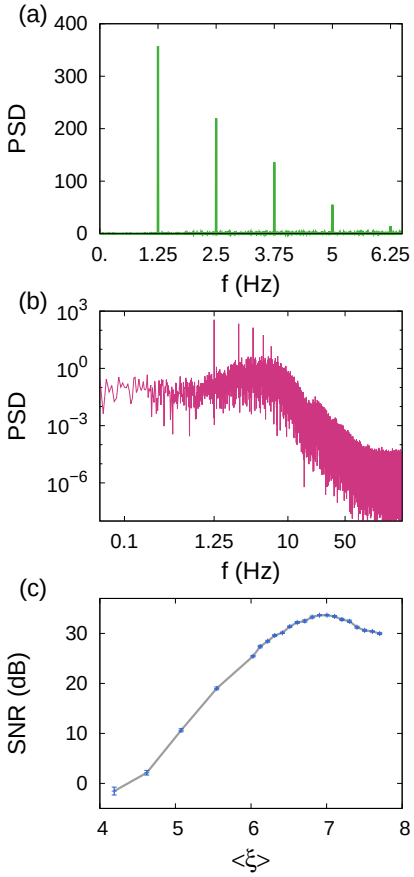

FIG. 6. (Color online) Power spectral density (PSD) of the cortical model in which a small fraction ($g_s = 0.1$) of excitatory neurons is stimulated by a sinusoidal signal (Eq. (9)) with frequency $f_s = 1.25$ Hz in the presence of sensory noise with $\langle\xi\rangle = 7.0$. (a) PSD versus the frequency f, linear scale; (b) PSD versus f, log-log scale. (c) Signal-to-noise (SNR) ratio versus $\langle\xi\rangle$. SNR is in decibel $[10\log_{10}(SNR)]$. Parameters in simulations are the same as in Fig. 2 and 5.

fluctuations plays a role of an additional noise that affects collective phenomena in interacting systems [31]. We discuss finite-size effects in Sec. IV B.

IV. SIGNAL DETECTION IN MODULAR NEURONAL NETWORKS

In the brain, neurons of similar function are grouped together in columns (or modules). This kind of organization assumes that synaptic connections are arranged denser within columns and sparser between columns. The columnar organization of the neocortex has been documented in studies of sensory and motor areas in many species [43–45]. Cortical columns are formed by the binding of many minicolumns (their number varies between 50 and 80) by common input and short range horizontal connections [45]. Understanding the role of modular organization (community structure, clustered

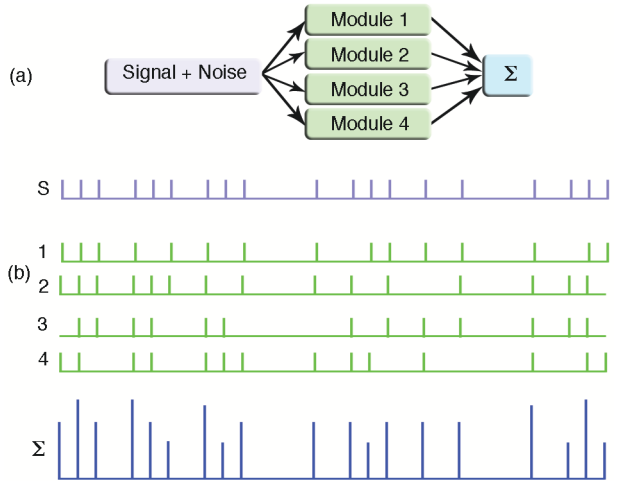

FIG. 7. (Color online) Signal detection in neuronal networks with modular structure from numerical integration of Eq. (3). (a) A signal together with noise is delivered to four modules 1, 2, 3 and 4. Responses of these modules are averaged in a module denoted as Σ. (b) S represents the signal 'ola' sent to these four modules. This signal with noise generates output signals 1, 2, 3 and 4 from the respective modules. The signal Σ represents the average over the output signals.

networks) is an open problem in neuroscience [46, 47].

In this section we show by use of numerical integration and simulations that the signal recognition in the regime with SR may be remarkably improved if a neuronal network has a modular organization similar to the partition of columns into minicolumns. We consider a neuronal network in which N neurons are grouped in n modules of size N/n. These modules are described by the cortical model in Sec. II and act in the regime of SR. A modular system is shown schematically in Fig. 7(a). All modules receive signal+noise inputs. Signals are represented by trains of pulses instead of periodic signals. Then the responses of the modules are summed up and averaged.

A. Detection of pulsed signals in numerical integration

The sinusoidal signal in Fig. 2(a) carries no information. Let us consider a case when a sensory signal contains information. We choose the message 'ola' ('hello' in Portuguese) expressed in Morse code as the digital code, 11101110111000101110101000101111. In order to represent this message as a sensory signal, we consider rectangular pulses separated by a time interval equal to 235 ms (the period of the sustained network oscillations of 5.2 Hz). The duration of these pulses was chosen about 30 ms that is about 8 times smaller than the period of network oscillations. The number of these pulses equals the number of bits in our message. Finally, we remove pulses corresponding to zeros. As a result we obtain a sensory signal representing our message 'ola' (see Fig. 7). De-

spite the pulse amplitude was chosen sufficiently small, every pulse can generate with a certain probability a single sharp oscillation in a module. Figure 7 shows that the response of the modules to this message is stochastic even at the optimal level of sensory noise. On one hand, the module does not detect some pulses. On the other hand, it may elicit 'false' responses. For given network parameters, sensory noise level, and signal's amplitude, we measured the probability p that a pulse in the signal is detected in a module, i.e., the pulse generates a single sharp oscillation. For the parameters chosen in our model and the signal's amplitude $A_s = 0.0135$, numerical integration of Eq. (3) gives $p \approx 5/7$. Alternatively, one can say that two pulses of seven may be missed or may be 'false'. In our numerical integration of Eq. (3) we assume that all modules receive the same signal+noise input (note that apart the sensory noise there is also intrinsic synaptic noise in every module). This method is similar to the stimulation of neuronal networks by an electric field as in [9]. Then, responses of the modules to the sensory signal are combined and we obtain an averaged response as shown in Fig. 7. For every pulse in the message 'ola', the probability that at least one of the modules detects it is

$$\Pi(n) = 1 - \prod_{m=1}^{n} (1 - p_m), \tag{11}$$

where p_m is the probability that the module with index $m = 1, ..., n$ detects a pulse. If the modules have the same probability $p_m = p$, then $\Pi(n)$ increases with increasing the number of modules n as $\Pi(n) \approx np$ at $p \ll 1$. In turn, the probability of an error, $1 - \Pi(n)$, decreases exponentially with increasing n as $1 - \Pi(n) = \exp[-n|\ln(1-p)|]$. If we want to detect every pulse of the message with probability of, say, 99%, then the necessary number n of modules can be found from the condition $\Pi(n) = 0.99$ (see, for example, Ref. [48]). For the obtained $p \approx 5/7$, Eq. (11) gives $n = 4$. The response to the message 'ola' averaged over 4 neuronal modules is shown in Fig. 7. This result illustrates that modular structures improve remarkably the detection of weak signals.

B. Simulations of modular networks

In our simulations of modular networks, $N = 50400$ neurons were grouped in n modules of size $N_m = N/n$, $n = 1, 2, \ldots, 50$. The modules are bound together by a common input but there are no connections between modules. The modules have the same structure as the random networks described in Sec. II. We used a train of random pulses obtained from a periodic pulse train by the removal of pulses with probability 40%. The pulse duration was $W = 0.2$ s, the amplitude $A_s = 4.5$, and the pulse rate $f = 0.75$ Hz. The pulsed signal was delivered to the modules together with sensory noise (normally distributed random spikes with the mean number $\langle \xi \rangle = 5.7$ of spikes per integration time, and the variance $\sigma_s^2 = 5$). We used two stimulation methods. In both methods, we chose at random a small fraction, $g_s = 10\%$, of excitatory neurons in each module. In the first method, every chosen neuron received independent sensory noise together with the pulsed signal. In the second method, the pulsed signal was delivered with the same noise to all chosen neurons. While the first method takes into account the synaptic noise in sensory systems, the second method mimics the stimulation of neuronal networks by an electric field that acts simultaneously on many neurons as in [9]. Analyzing dynamics of the network during a large observation time (80 s), we found the probability p_m that a signal's pulse is detected by a module with index $m = 1, \ldots, n$ of size N/n (a pulse is detected if it evokes a sharp large-amplitude network oscillation during a time interval equal to twice the pulse duration after the signal's pulse begins). Averaging p_m over 10 network realizations, we found the average probability $p(n)$ shown in Fig. 8(a) for the two stimulation methods. Using the first stimulation method (uncorrelated sensory noise), we observed that $p(n)$ first increases, meaning that the excitability of the modules increases. After reaching a maximum, $p(n)$ decreases. Using the second stimulation method (correlated sensory noise), we observed a monotonic decrease of $p(n)$ with decreasing the module size. Since, except the module size, all model parameters were fixed in our simulations for uncorrelated and correlated noise, we believe that the observed decrease of $p(n)$ at large n is mainly due to finite-size effects. Finite-size fluctuations are expected to increase as n increases and disrupt collective oscillations in the neuronal networks.

We also suggest that the peak of the function $p(n)$ observed at $n = 10$ in the case of uncorrelated noise may be caused by a competition between the increase of mod-

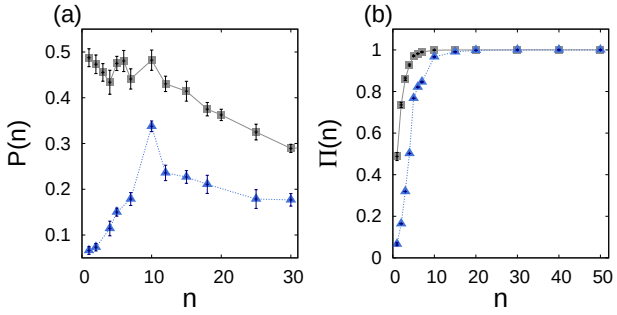

FIG. 8. (Color online) (a) Probability $p(n)$ that a signal's pulse is detected by a module of size N/n versus n ($N = 50400$ in our simulations). (b) Probability $\Pi(n)$ of the signal detection in a network with n modules. In panels (a) and (b), symbols represent results of two stimulation methods: (1) each neuron in every module receives independent sensory noise but the same pulsed signal (triangles); (2) neurons in the modules receive the same sensory noise and the same pulsed signal (squares). Parameters of the signal+noise input are in the text. Other parameters are the same as in Figs. 2 and 5.

ule excitability and suppression of collective oscillations as n increases. The large values of $p(n)$ observed in the case of correlated noise (see Fig. 8(a)) may be due to the fact that the correlated noise results in correlations between neuronal activities of modules. As one can expect, these correlations increase $p(n)$ in comparison to the case of uncorrelated noise. However, it is unclear how these correlations together with finite-size effects are responsible for the observed monotonic decrease of $p(n)$ as n increases in the case of correlated noise, in contrast to the non-monotonic behavior of $p(n)$ observed in the case of uncorrelated noise.

Figure 9 shows that when the module size decreases, sharp network oscillations evoked by signal's pulses lose their deterministic shape and strongly vary in amplitude. Unfortunately, the mechanism of this effect is unknown. It may be due to an increase of the clustering coefficient when size N_m of the modules decreases. Neglecting the directness of connections between neurons, we can estimate the clustering coefficient characterizing the occurrence of triangles in the network structure. The clustering coefficient is c/N_m, where c is the mean degree (size dependence of structural properties of complex networks and the role of triangles in network dynamics are discussed in the review [32]). Appearance of numerous triangles may destroy the balance between excitation and inhibition. Note that standard statistical analysis shows that the scale of stochastic activity fluctuations in a network of size N_m is $O(1/N_m^{1/2})$ (see, for example, [42]).

Finally, we found the probability $\Pi(n)$, using Eq. (11) and averaging over the observation time. As one can see in Fig. 8(b)), $\Pi(n)$ increases with increasing the number of modules n for both stimulation methods. Interestingly, at large n, even though $p(n)$ decreases, $\Pi(n)$ remains large, meaning that the large number of modules compensates the decrease of $p(n)$. Therefore, the fragmentation of the neuronal system into several modules increases the reliability of signal detection.

Now we compare our model of interacting neurons with the summing network [22] of noninteracting neurons. In the summing network, neurons receive common input and act in parallel. In our model, neurons are grouped in modules receiving common input and working in parallel. If the same fraction g_a of neurons in both models is initially activated by a signal, then in the summing network their outputs are summed while in our model they activate other neighbors, forming sharp spikes of neuronal activity in the modules. Every spike involves about 90% of the neurons in a module independently of g_a if g_a is at least about 0.01 (at $\langle n \rangle = 16$). Thus, the output from the modules can be $0.9/g_a \approx 90$ times larger than the one in the summing network. Note that our model is best suited for detecting low frequency signals, whereas the summing network recognizes high frequency signals (since our model uses network oscillations, whereas neurons in the summing network can generate action potentials with higher frequency than network oscillations).

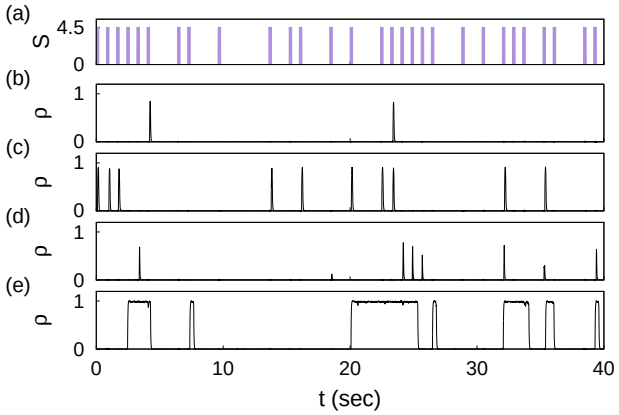

FIG. 9. (Color online) (a) A train of random rectangular pulses as a sensory signal. Panels (b)-(e) show stimulated neuronal activity of one of n modules of size $N_m = N/n$ for $N = 50400$: (b) $n = 2$ ($N_m = 25200$); (c) $n = 10$ ($N_m = 5040$); (d) $n = 30$ ($N_m = 1680$); (e) $n = 40$ ($N_m = 1260$). Neurons receive independent sensory noise together with the signal. Other parameters are the same as in Fig. 8.

V. CONCLUSION

In this paper, we demonstrated stochastic resonance in the response of neuronal networks to sinusoidal signals in the presence of sensory noise and intrinsic synaptic noise. We also showed that SR together with modular structure can remarkably improve signal detection. Our simulations of the cortical model with stochastic neurons and numerical integration of rate equations revealed that sensory noise can enhance response of neuronal networks to sinusoidal and non-periodic pulsed signals. We demonstrated this noise-enhanced response in the case of neuronal networks that are in a dynamical state near a saddle-node bifurcation corresponding to the appearance of sustained network oscillations. In this state, neuronal networks have a remarkable excitability. Even a subthreshold sensory input delivered to a small fraction of excitatory neurons can evoke a sharp large-amplitude oscillation of neuronal activity synchronized with some degree of correlation with the signal. These sharp oscillations are nonlinear events that represent a strongly synchronized activity of a large fraction of neurons (90% of neurons in our model) and have a deterministic shape. We found that the signal-to-noise ratio reaches a maximum at an optimum level of sensory noise, manifesting stochastic resonance. The important feature of our mechanism is that this mechanism is universal and does not qualitatively depend on the underlying model. SR has a collective nature due to interaction between neurons, rather than just due to excitable dynamics of single neurons as in models [6, 10, 11, 19, 21]. Therefore, breaking of cooperation between neurons results in suppression of this mechanism. Indeed, we observed suppression of signal detection by finite-size effects. However, these effects play no role for single neuron dynamics.

Using our model, we mimicked the experiments of Gluckman *et al.* [9] who observed SR in hippocampal slices from mammalian brain. Results of our numerical analysis qualitatively agree with the experiments. This evidences that the phenomena observed in [9] may have collective nature. It also supports the suggestion that SR may enhance effects of weak hippocampal theta or more widespread gamma oscillations within the brain.

We suggest that the network response represented by a strongly synchronized activity of a large fraction of neurons can also play an important role in various mechanisms of signal processing in the brain. The fact that the sharp oscillations have a deterministic form and can be evoked by a small group of neurons may be of crucial importance not only for signal detection, but also for information transmission and communication between different areas of the brain. This mechanism enables a small group of neurons to control a large neuronal network.

In order to show the role of modular organization in signal detection, we considered networks in which neurons are grouped in modules working in the regime of SR. Using numerical integrations and simulations of the cortical model, we demonstrated that even a few modules can strongly enhance the reliability of signal detection in comparison with the case when a modular organization is absent.

One can note the following important properties of our model: (1) the amplification of subthreshold signals can be regulated by a flow of spikes from other brain areas; (2) a sensory signal can be delivered to a small fraction (we used 10%) of neurons without a lost in the output signal; (3) neurons in our network use for its own benefit not only sensory noise but also internal synaptic noise; (4) grouping of neurons into modules improves signal detection.

VI. ACKNOWLEDGEMENTS

This work was partially supported by FET IP Project MULTIPLEX 317532, the project PEst-C / CTM / LA0025 / 2011, and the project 'New Strategies Applied to Neuropathological Disorders,' cofunded by QREN and EU. K. E. L. and M. A. L. were supported by the FCT Grants No. SFRH/ BPD/ 71883/2010 and No. SFRH/ BD/ 68743 /2010.

[1] G. B. Ermentrout, R. F. Galn, and N. N. Urban, Trends Neurosci. **31**, 428 (2008).
[2] A. Faisal, L. Selen, and D. M. Wolpert, Nat. Rev. Neurosci. **9**, 292 (2008).
[3] M. D. McDonnell and L. M. Ward, Nat. Rev. Neurosci. **12**, 415 (2011).
[4] L. Gammaitoni, P. Hänggi, P. Jung, and F. Marchesoni, Rev. Mod. Phys. **70**, 223 (1998).
[5] J. K. Douglass, L. Wilkens, E. Pantazelou, and F. Moss, Nature **365**, 337 (1993).
[6] K. Wiesenfeld and F. Moss, Nature (London) **373**, 33 (1995).
[7] J. E. Levin and J. P. Miller, Nature **380**, 165 (1996).
[8] D. F. Russell, L. A. Wilkens, and F. Moss, Nature **402**, 291 (1999).
[9] B. J. Gluckman, T. I. Netoff, E. J. Neel, W. L. Ditto, M. L. Spano, and S. J. Schiff, Phys. Rev. Lett. **77**, 4098 (1996).
[10] W. C. Stacey and D. M. Durand, J. Neurophysiol. **83**, 1394 (2000).
[11] W. C. Stacey and D. M. Durand, J. Neurophysiol. **86**, 1104 (2001).
[12] I. Hidaka, D. Nozaki, and Y. Yamamoto, Phys. Rev. Lett. **85**, 3740 (2000).
[13] T. Mori and S. Kai, Phys. Rev. Lett. **88**, 218101 (2002).
[14] K. Kitajo, D. Nozaki, L. M. Ward, and Y. Yamamoto, Phys. Rev. Lett. **90**, 218103 (2003).
[15] L. Ward, Contemp. Phys. **50**, 563 (2009).
[16] L. M. Ward, S. E. MacLean, and A. Kirschner, PLoS ONE **5**, e14371 (2010).
[17] R. Benzi, G. Parisi, A. Sutera, and A. Vulpiani, Tellus **34**, 10 (1982).
[18] H. Gang, T. Ditzinger, C. Ning, and H. Haken, Phys. Rev. Lett. **71**, 807 (1993).
[19] K. Wiesenfeld, D. Pierson, E. Pantazelou, C. Dames, and F. Moss, Phys. Rev. Lett. **72**, 2125 (1994).
[20] W. J. Rappel and S. H. Strogatz, Phys. Rev. E **50**, 3249 (1994).
[21] A. Longtin, Phys. Rev. E **55**, 868 (1997).
[22] J. J. Collins, C. C. Chow, and T. T. Imhoff, Nature **376**, 236 (1995).
[23] M. D. McDonnell, N. G. Stocks, and D. Abbott, Phys. Rev. E **75**, 061105 (2007).
[24] D. R. Chialvo, A. Longtin, and J. Müller-Gerking, Phys. Rev. E **55**, 1798 (1997).
[25] M. Perc, Phys. Rev. E **76**, 066203 (2007).
[26] Q. Wang, M. Perc, Z. Duan, and G. Chen, Chaos **19**, 023112 (2009).
[27] Y. Gong, M. Wang, Z. Hou, and H. Xin, Chem. Phys. Chem. **6**, 1042 (2005).
[28] M. Ozer, M. Perc, and M. Uzuntarla, Phys. Lett. A **373**, 964 (2009).
[29] M. Yoshida, H. Hayashi, K. Tateno, and S. Ishizuka, Neural Networks **15**, 1171 (2002).
[30] K.-E. Lee, M. A. Lopes, J. F. F. Mendes, and A. V. Goltsev, Phys. Rev. E **89**, 012701 (2014).
[31] K. Binder, Ferroelectrics **73**, 43 (1987).
[32] S. N. Dorogovtsev, A. V. Goltsev, and J. F. F. Mendes, Rev. Mod. Phys. **80**, 1275 (2008).
[33] A. V. Goltsev, F. V. de Abreu, S. N. Dorogovtsev, and J. F. F. Mendes, Phys. Rev. E **81**, 061921 (2010).
[34] M. Benayoun, J. D. Cowan, W. van Drongelen, and E. Wallace, PLoS Comput. Biol. **6**, e1000846 (2010).
[35] E. Wallace, M. Benayoun, W. van Drongelen, and J. D. Cowan, PLoS ONE **6**, e14804 (2011).
[36] H. R. Wilson and J. D. Cowan, Biophys. J. **12**, 1 (1972).
[37] H. Wilson and J. Cowan, Kybernetik **13**, 55 (1973).
[38] D. J. Amit and N. Brunel, Cereb. Cortex **7**, 237 (1997).

[39] S. Fujisawa, N. Matsuki, and Y. Ikegaya, J. Physiol. **561**, 123 (2004).
[40] M. L. Molineux, F. R. Fernandez, W. H. Mehaffey, and R. W. Turner, J. Neurosci. **25**, 10863 (2005).
[41] A. Bragin, G. Jandó, Z. Nádasdy, J. Hetke, K. Wise, and G. Buzsáki, J. Neurosci. **15**, 47 (1995).
[42] C. W. Gardiner, *Handbook of stochastic methods for physics, chemistry and the natural sciences*, 3rd ed., Springer Series in Synergetics, Vol. 13 (Springer-Verlag, Berlin, 2004).
[43] V. B. Mountcastle, A. L. Berman, and P. W. Davies, Am. J. Physiol. **183**, 646 (1955).
[44] D. H. Hubel and T. N. Wiesel, J. Physiol. **160**, 106 (1962).
[45] V. B. Mountcastle, Cereb. Cortex **13**, 2 (2003).
[46] A. Litwin-Kumar and B. Doiron, Nat. Neurosci. **15**, 1498 (2012).
[47] M. D. McDonnell and L. M. Ward, PloS ONE **9**, e88254 (2014).
[48] B. A. Carlson, P. B. Crilly, and J. Rutledge, *Communication Systems* (McGraw-Hill, New York, 2001).